The Impact of Abstract-Modelled Wall Layouts on User Throughput in Wireless Indoor Environments

Viktor Stoynov[1] and Zlatka Valkova-Jarvis[2]

Abstract – **In this work, the performance of indoor users' throughput is studied through the abstract modelling of walls. A new blockage object arrangement is introduced and compared with existing abstract-modelled blockage arrangements to demonstrate its improved representation of real-life scenarios. Ten different scenarios are defined, combining different wall layouts and transmitter dispositions. The scenarios represent possible real working environment sites and are experimentally tested for different number of receivers.**

Keywords – **Indoor environment, wireless communications, blockage modelling, user throughput**

I. INTRODUCTION

Demands on wireless data traffic have increased dramatically in recent years, due to user requirements for higher data rates and excellent coverage in indoor environments. The trend suggests that the number of people living in urban areas will increase dramatically in the next few years.

One of the main problems facing telecommunication networks is how to provide an excellent service to users located at the periphery of the serving cell. These users are subjected to significant interference from neighbouring base stations and, in the case of wireless indoor environments, from adjacent transmitters (*Tx*). One major obstacle in enclosed spaces is the wall layout: walls, as blockage objects, mitigate interference but also cause the signal to deteriorate, thus worsening the quality of the mobile services provided. Good indoor coverage depends to a large extent on the femtocells' location. The signals from non-serving transmitters permeate the wall and fade easily, hence they are not a source of interference.

Abstract modelling of indoor obstacles is often neglected and the enormous influence of wall layout on signal propagation is thus overlooked in the research. Some recent works [1], [2], [3] have developed and investigated abstract models of indoor communication environments, and considered the major parameters of signal obstacles, such as length, attenuation level, density allocation, etc. Analytical expressions of the average attenuation of signals passing through walls are derived and system-level simulations performed to demonstrate the impact of the walls and transmitter devices arrangement on the Signal-to-Interference Ratio (SIR) and users' throughput.

In this paper a new, more realistic abstract-modelled wall layout is developed. It demonstrates clear advantages when compared experimentally to previously-developed similar abstract models. Furthermore, ten scenarios, consisting of four different types of wall distributions and free space propagation, are composed. The abstract wall generation methods use the same wall density, aiming to achieve lucid conclusions after the direct comparison of users' throughputs. The experimental set uses the same enclosed space (Region of Interest - RoI), number of *Tx*, transmitter distance and power, while the number of users (receivers - *Rx*) varies.

II. SYSTEM MODEL

A. Abstract wall layouts generation methods

In this work, four methods for wall arrangement are considered (Fig. 1). The first wall generation method is based on a Boolean scheme, where the positions of the centre points of the walls are randomly distributed according to a *Poisson Point Process* (PPP) of *density* λ. The lengths of the walls follow *Arbitrary Distribution* $f_L(l)$. The disposition of the walls is either parallel or at right-angles, which defines a two-state wall layout, realised when the angle between any two walls is a binary choice – $\{0; \pi/2\}$. This abstract wall generation method is denoted as **[binary]** (Fig. 1a).

The wall distribution, generated by a Manhattan grid of equidistantly-spaced walls is named **[regular]** (Fig. 1b). It is assumed that the walls are oriented perpendicular to the coordinate axes. The space between every two adjacent parallel walls is set to a constant Δ. This distance is calculated based on the dimensions of the considered RoI and is related to the *average wall length* $E[L]$ and *wall density parameter* λ: $\Delta=2/\lambda E[L]$. Geometrically, the RoI is a rectangle or square with sides of length – integer which is a multiple of Δ. In order to achieve different realisations of the **[regular]** wall layout, Δ might be randomly shifted by δ_x in the *x*-axis and by δ_y in the *y*-axis.

The third abstract wall generation method is obtained by two *Manhattan Line Processes* (MLP) and is named after it - **[MLP]** (Fig.1c). This method is very similar to the **[regular]**, but differs in that the wall distance Δ is not a constant but a variable. The **[MLP]** method reproduces the most realistic indoor environments, compared to the **[binary]** and **[regular]** wall layouts.

In this publication, a new method of wall layout is proposed (Fig.1d). It is named Realistic Indoor Environment Generator [**RIEG**] and consists of the following steps:

- Positioning of rectangles in a predefined area – RoI;

[1]Viktor Stoynov is with the Faculty of Telecommunications at Technical University of Sofia, 8 Kl. Ohridski Blvd, Sofia 1000, Bulgaria, E-mail: vstoynov@tu-sofia.bg.

[2]Zlatka Valkova-Jarvis is with the Faculty of Telecommunications at Technical University of Sofia, 8 Kl. Ohridski Blvd, Sofia 1000, Bulgaria. E-mail: zvv@tu-sofia.bg.

- The coordinates of the starting point of each rectangle are selected randomly. The sides of the rectangle are then plotted, ensuring that the rectangle remains within the RoI;
- The total length of the walls takes into account the value of the wall density parameter. Hence, different methods for wall arrangement can be compared;
- The confined spaces, resulting from the rectangles' distribution, result in a more realistic indoor design compared to the other three methods.

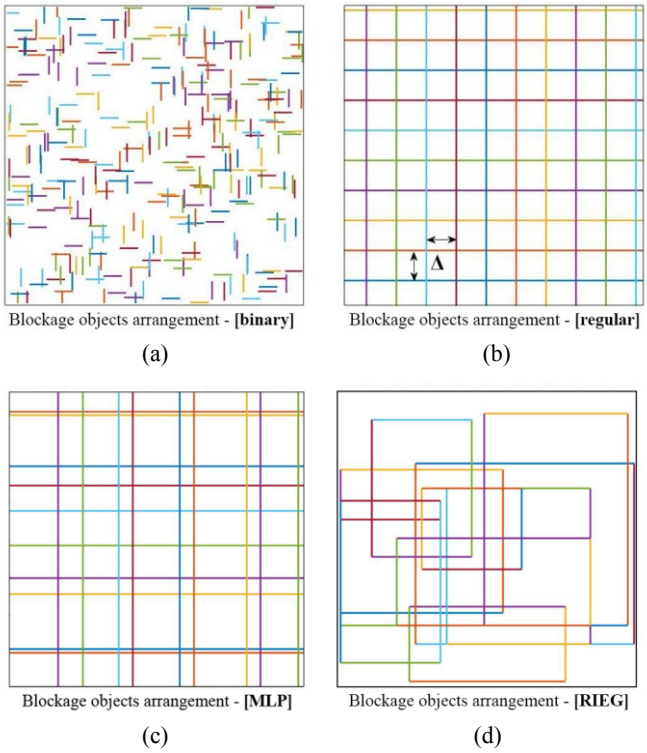

Fig.1. Generated wall maps for (a) **[binary],** (b) **[regular],** (c) **[MLP]** and (d) **[RIEG]** cases

There are also scenarios where no walls are distributed – **[free space]**. Thus, the experimental results can show how the existence of walls affects the level of user throughput.

B. Transmitter and receiver location

Four *Tx* in the indoor system model are located in the four corners of a square with side-length *R*, marked as **[square]** in the scenarios' descriptions (Fig. 2a). When the **[square]** transmitters are rotated by π/4, the alternative transmitters' location is obtained; this is labelled as **[rhomboid]** and is shown in Fig. 2b. When the simulations are performed without blockages, the location of the transmitters does not significantly affect the throughput of the receivers (*Rx*).

The receivers (users) are located at the cell edge, at a distance of *R*/2 from the closest transmitter. This transmitter is defined as the *desired transmitter* – (*dTx*). The other three transmitters are assumed to be *sources of interference* ($iTx_{1\div3}$). The location of each receiver is determined by its polar coordinates (*R*/2, Φ), measured against the nearest transmitter. The angle Φ ranges from 0 to π /2 (Fig. 2).

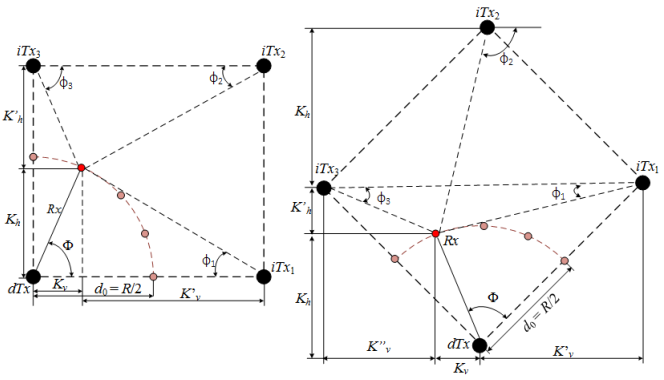

Fig.2. Transmitters (*Tx*) and receivers (*Rx*) location (a) **[square]** and (b) **[rhomboid]**

C. Scenario setups

Combining the location of the transmitters and wall layouts, the following ten scenarios are defined:

S1 = {[binary], [square]}
S2 = {[binary], [rhomboid]}
S3 = {[regular], [square]}
S4 = {[regular], [rhomboid]}
S5 = {[MLP], [square]}
S6 = {[MLP], [rhomboid]}
S7 = {[free space], [square]}
S8 = {[free space], [rhomboid]}
S9 = {[RIEG], [square]}
S10={[RIEG], [rhomboid]}

D. Signal propagation characteristics

The downlink signal is assumed to experience attenuation due to the wall blockages, distance-dependent path loss and small-scale fading. The *path loss law l(d)* is defined by the equation:

$$l(d) = \frac{1}{c} d^{-\alpha}, \qquad (1)$$

where *d* is the distance between a transmitter and a receiver; *c* is a constant equal to 38.46 dB when using femtocells; and α is the path loss exponent with a value of 2 [4].

The attenuation caused by the walls is determined by accumulating the attenuation of each wall. In the models considered in this work, the blockages are defined as two-dimensional objects, and the investigated wireless network is designed to be interference limited.

III. Analytical Model

One of the most important parameters is the average number of blockages *E*[*K*] that obstruct the path between the *Tx* and the *Rx*:

$$E[K] = \beta d . \qquad (2)$$

β is blockage factor that differs according to the wall distribution method. For the **[binary]** case it is:

$$\beta = \lambda E[L] \frac{\left(|\sin(\phi)| + |\cos(\phi)|\right)}{2}. \quad (3)$$

ϕ denotes the angle of the link between transmitter and receiver against the x-axis.

The average number of blockages $E[K]$ along a link with length d, can be expressed via equations (2) and (3). For the **[binary]** case this can be expressed as:

$$E[K] = \lambda E[L] d \frac{\left(|\sin(\phi)| + |\cos(\phi)|\right)}{2}. \quad (4)$$

It is clear that the average number of blockages $E[K]$ located between a *Tx* and a *Rx* is directly proportional to the average length of these wall objects $E[L]$.

For the **[regular]** case, $E[K]$ is calculated as:

$$E[K] = N_x + N_y + p_x + p_y, \quad (5)$$

where N_x and N_y denote the number of walls without random shifts δ_x or δ_y, while p_x and p_y are the number of additional walls (new walls, required to preserve the average wall density, after a random shifting is performed).

When the number of walls is set to K_i, the total attenuation of the signals in the area will be $\omega_i = \omega^{Ki}$. Although each wall may have a different attenuation, the experiments conducted here consider 10 dB fixed attenuation. Thus the SIR for one indoor user can be:

$$\gamma = \frac{P_0 h_0 l(d_0) \omega_0}{\sum_{i=1}^{3} P_i h_i l(d_i) \omega_i}, \quad (6)$$

where d_o is the distance between the receiver *Rx* and its serving (desired) transmitter *dTx*, P_0 is the transmit power of *dTx*, while P_i (i = 1, 2, 3) are the power of the interfering transmitters iTx_1, iTx_2 and iTx_3, respectively. h_0 and h_i denote the small-scale fading, d_i is the distance between the receiver and the i-th interfering transmitter and $l(d_0)$ and $l(d_i)$ are the path losses.

In [1] an analytic expression to approximate *geomean* (γ) for the **[binary]** case is derived. The average SIR is calculated by:

$$geomean(\gamma) \approx \int_{-\infty}^{\infty} \left(\frac{d}{d\delta} \left(1 - \prod_{i=1}^{3} \frac{1}{1 + \delta \frac{\overline{\omega}_i'}{\overline{\omega}_0} \frac{l(d_i)}{l(d_0)}} \right) \Bigg|_{\delta = t} \right) t \, dt. \quad (7)$$

$\overline{\omega}_i'$ provides an accurate approximation for *geomean* (ω_i) and is called *effective wall attenuation*.

For **[MLP]** the SIR is calculated by splitting the line-processes into the horizontal and vertical processes (Fig. 2a) [2]. For the **[square]** case, the SIR is calculated by:

$$\gamma = \frac{h_0 d_0^{-\alpha} \omega^{K_v + K_h}}{h_1 d_1^{-\alpha} \Omega_{sq\_1} + h_2 d_2^{-\alpha} \Omega_{sq\_2} + h_3 d_3^{-\alpha} \Omega_{sq\_3}}, \quad (8)$$

where:

$$\Omega_{sq\_1} = \omega^{K'_v + K_h}; \quad \Omega_{sq\_2} = \omega^{K'_v + K'_h}; \quad \Omega_{sq\_3} = \omega^{K_v + K'_h}. \quad (9)$$

K_v and K_h are the wall counts between any user and the *dTx* and K'_v and K'_h are the wall counts between the user and the interfering transmitters iTx_1, iTx_2, iTx_3 (Fig. 2a). They all are *Poisson Random Variables*.

For the **[rhomboid]** case (Fig. 2b), the SIR is defined by the equation:

$$\gamma = \frac{h_0 d_0^{-\alpha} \omega^{K_v + K_h}}{h_1 d_1^{-\alpha} \Omega_{rh\_1} + h_2 d_2^{-\alpha} \Omega_{rh\_2} + h_3 d_3^{-\alpha} \Omega_{rh\_3}}, \quad (10)$$

where

$$\Omega_{rh\_1} = \omega^{K'_v + S(-\cos(\phi)) K_v + K'_h}; \quad \Omega_{rh\_2} = \omega^{K_v + K'_h + K''_h}; \quad \Omega_{rh\_3} = \omega^{K''_v + S(-\cos(\phi)) K_v + K'_h}. \quad (11)$$

K''_v and K''_h denote the wall counts between any user and the interferers iTx_1, iTx_2, iTx_3 as is shown in Fig. 2b.

IV. System-level simulations and results

A. Setup

The four transmitters are spaced a distance of R=40m apart regardless of the pattern of their arrangement - **[square]** or **[rhomboid]**. Each *Tx* is defined as a femtocell with a transmit power of 100mW. The distance between the *dTx* and the receivers is set to 20 m. The wall density is λ=0.05 m^{-2}, the average wall length is $E[L]$=5m and the wall attenuation is set to 10 dB for each simulation. All parameters and their numerical values are given in Table 1.

TABLE I
PARAMETERS AND THEIR NUMERICAL VALUES

Parameter	Value
Inter transmitter distance	R=40 m
Number of interferers	3
Distance between *Tx* and *Rx* (radius)	R/2=20 m
Rx positions	5,15,25
Wall density	λ=0.05 m^{-2}
Wall attenuation	10 dB
Average wall length	$E[L]$=5m
Scenario realisations	10^5
Path loss law	$l(d)=10^{-38.46/10} d^{-\alpha}$
Transmitter power (femtocells)	P=100 mW

B. Average wall attenuation results

In order to compare the different wall arrangement models, the experiments are conducted under the same conditions - the average number of walls, receivers and transmitters remaining constant for each simulation.

The defined ten scenarios are simulated for different numbers of users - 5, 15, 25.

The average wall attenuation and SIR can be analytically calculated only for the **[binary]** wall distribution. The **[regular]** wall pattern scenarios can only be examined using simulations. The Vienna LTE-A system-level simulator [5] is a proper tool for an abstract modelling of the scenarios considered in this work. The results for users' throughput are obtained after 500 simulation runs – each with 200 identical transmission time intervals. The wall attenuation research conclusions result from 5000 simulations.

In [2] the wall attenuations for the different scenarios are determined. The **[binary]**, **[regular]** and **[MLP]** scenarios are analytically verified and it is shown that analytical results and simulation curves for the average attenuation level per transmitter match perfectly for both **[square]** and **[rhomboid]** transmitter layouts.

C. User throughput results

Fig. 3, 4 and 5 show the average throughput of each user when different numbers of *Rx* positions are used - 5, 15, 25 respectively.

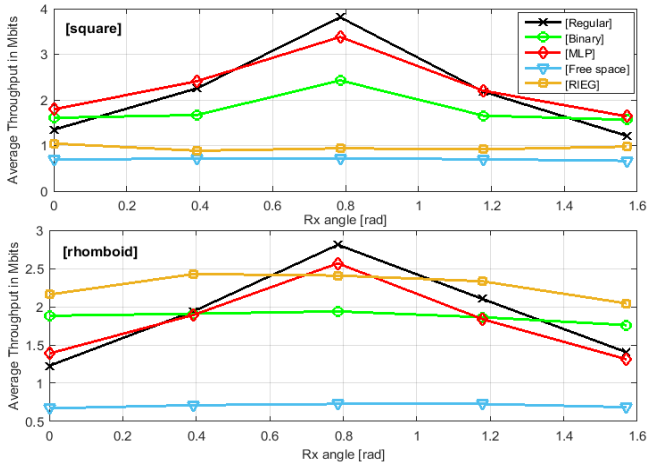

Fig.3. Average user throughput results for 5 users and **[square]** and **[rhomboid]** transmitter layouts

It is easy to see that when there are no walls in the RoI – **[free space]** scenarios, the average throughput for each user dramatically decreases, which proves the important role of obstacles in interference mitigation. When comparing the simulation results for **[square]** and **[rhomboid]** transmitter layouts and an equal number of users, the same values of the throughputs are obtained. The location layouts of transmitters and receivers lose relevance when there are no walls – scenarios **S7** and **S8**. The angular collocation of the receiving and transmitting devices affects the wireless network performance only when direct visibility is impaired due to wall obstruction.

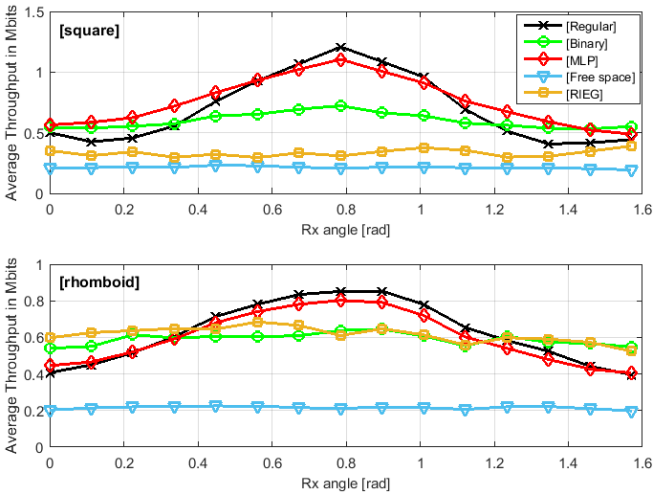

Fig.4. Average user throughput results for 15 users and **[square]** and **[rhomboid]** transmitter layouts

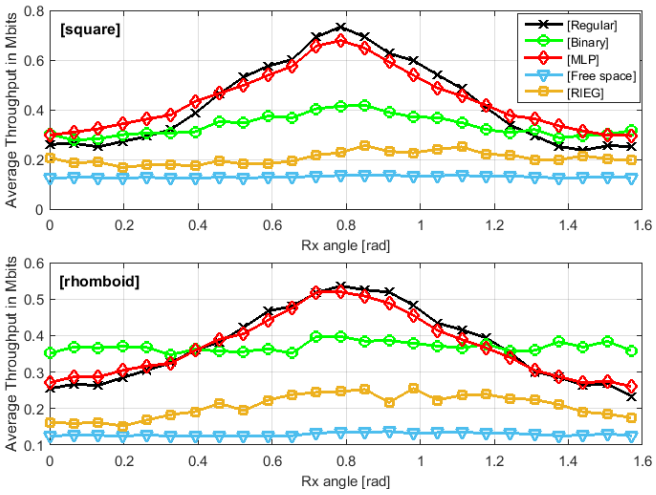

Fig.5. Average user throughput results for 25 users and **[square]** and **[rhomboid]** transmitter layouts

Apart from the users in the periphery of the femtocell, the graphs follow the same trend as reported in [2] results regarding SIR. The Manhattan grid-like wall arrangements, denoted as **[regular]** and **[MLP]**, show better performance, compared to the **[binary]** case, no matter how many *Rx* positions are explored. The explanation for this behaviour is that the walls located along the *y*-axis affect the signal propagation between the *dTx* and the users to a much lesser extent. These walls, however, are very important to suppress the interference from other transmitters ($iTx_{1\div3}$). The distribution of the walls in **[binary]** is much more difficult to predict compared to **[regular]** and **[MLP]**.

An interesting fact is that the **[MLP]** curves are very closely located to those for **[regular]** - something which is not observed in the figures for SIR. The reason for such behaviour is the identical number of walls for both generation methods although their wall layouts appear different. For the **[regular]** (Fig. 1b) wall layout – the distance between the walls is the same, while for **[MLP]** – it varies for every simulation (Fig. 1c). The reduction of the users' throughput which was observed in a part of the simulations for the **[MLP]** wall

layout is due to there being fewer obstacles between the *iRx* and $iTx_{1\div3}$ compared to those between *iRx* and the *dTx*. Conversely, the [**regular**] wall generation method provides roughly the same number of obstacles between users and the desired transmitter, and users and the interfering transmitters for each iteration.

An increase of throughput is observed for *Rx* positions around **Φ=π/4**, where the three interfering transmitters have an identically strong impact on the total interference. Obviously, the **[regular]** grid offers the best protection for users against interference.

The users located around **Φ=0** and **Φ=π/2** experience a surprisingly good throughput, especially in the **[binary]** case, as opposed to the trend of the SIR. At these positions, the **[square]** layout's main sources of interference are the nearest distributed transmitters – iTx_1 and iTx_3 respectively (Fig. 2). For the **[rhomboid]** transmitter location, the main sources of interference are even more numerous, since the receivers are closer to iTx_2. In contrast to the **[regular]** and **[MLP]** wall arrangements, which always contain obstacles between the *Rx* and the *dTx*, the **[binary]** layout provides fewer blockages to signal propagation, especially for user positions in **Φ=0** and **Φ=π/2**.

In the **[RIEG]** wall layout, when used with the transmitting devices in the **[square]** configuration, the leftmost- and rightmost-located users have the highest rate of data transmission, especially for 5 and 15 users. Unlike the **[regular]** and **[MLP]** methods providing strictly determinate locations for the walls, when the **[RIEG]** layout is used the walls between users and transmitters are always random in number. Ergo, the main sources of interference are hard to predict and change constantly. This all makes the **[RIEG]** method more realistic.

It turns out that in the **[square]** *Tx* location, users receive nearly equal quality of service. This resembles the results for the **[binary]** configuration. In the case of the **[square]** layout (scenario **S9**), interference is lower compared to the **[rhomboid]** transmitters location (scenario **S10**), due to the different angular co-location/orientation of the walls to the desired transceiver. Also, the **[square]** layout provides fewer walls between the *Rx* and *dTx*. Walls parallel to the y-axis remain invisible to *dTx*, which increases the throughput of the users located in positions **Φ=0** and **Φ=π/2**.

Logically, we may conclude that the more realistic the distribution of the walls used, the harder it becomes to predict their impact on user throughput.

V. Conclusion

In this work, simulation and analytical results for average wall attenuation and system-level simulation results evaluating the average users' throughput are presented. Ten scenarios are composed and investigated determined by four different wall layouts and two different transmitter locations.

The experimental results for average user throughput obtained via system-level simulations show the same trends as the SIR performance [2]. It turns out that, due to different wall arrangements, the average wall attenuation and average throughput are angularly dependent. This is also the reason for the different performance of the two types of transmitter distributions. When no walls are used, i.e. free space of signal propagation is taken into account, the specific transmitter arrangement does not influence the average throughput of the users. Using the same amount of physical resources in each scenario while increasing the number of users leads to a decrease in average user throughput. The higher the number of users, the stronger the impact of the limited amount of physical resources becomes and the less the impact of wall-angle distribution. So, it is important when simulating different scenarios for each user to have the same amount of resources available, regardless of how many users are active.

In the present work it is also shown that the existence of walls between the users and transmitters mitigates the adverse influence of interference and leads to better coverage. However, if the number of walls, i.e. the average wall density, increases that would lead to degradation of the service. The wall distribution models can be used to achieve more realistic indoor environments in order to test different techniques for interference mitigation. The closest to a real-world scenario is the new **[RIEG]** wall arrangement method proposed in this work, which is realistic enough to be used as an indoor environment to test interference suppression techniques.

Future work may focus on modelling signal reflections in an indoor environment, where the walls have different attenuation and the transmitters and receivers are distributed according to stochastic geometry. Furthermore, improvements have to be made to RIEG to incorporate more realistically-located blockages and thereby to make the process more easily controlled by the designer. The influence of different parameters used in the simulations, such as transmission mode and channel model on the interference levels have to be extensively studied. It would also be interesting to investigate scenarios where the mmW indoor communication environment is taken into account.

Acknowledgement

This work was supported by the Scientific Project No.162ПД0011-07 of Technical University – Sofia, Bulgaria.

References

[1] M. Müller, M. Taranetz, V. Stoynov, M. Rupp. "Abstracting Indoor Signal propagations: Stochastic vs. Regular", 58th International Symposium ELMAR-2016, Zadar, Sept. 2016.

[2] M. Müller, M. Taranetz, and M. Rupp, "Analyzing Wireless Indoor Communications by Blockage Models," in IEEE Access, Volume PP, Issue 99, Dec. 2016.

[3] V. Stoynov. Investigation of Indoor Wireless Communication Environment Using Abstract Modelling, E+E (accepted)

[4] 3rd Generation Partnership Project (3GPP), "Evolved Universal Terrestrial Radio Access (E-UTRA); Further advancements for E-UTRA physical layer aspects," 3rd Generation Partnership Project (3GPP), TR 36.814, Mar. 2010.

[5] M. Rupp, S. Schwarz, and M. Taranetz, The Vienna LTE Advanced Simulators: Up and Downlink, Link and System Level Simulation, 1st ed., ser. Signals and Communication Technology. Springer Singapore, 2016.